Journal of Mathematical Biology (2024) 88:42
https://doi.org/10.1007/s00285-024-02063-2

Mathematical Biology

Effects of whaling and krill fishing on the whale–krill predation dynamics: bifurcations in a harvested predator–prey model with Holling type I functional response

Qin Pan[1] · Min Lu[1] · Jicai Huang[1] · Shigui Ruan[2]

Received: 23 August 2023 / Revised: 5 February 2024 / Accepted: 11 February 2024 /
Published online: 6 March 2024

Abstract

In the Antarctic, the whale population had been reduced dramatically due to the unregulated whaling. It was expected that Antarctic krill, the main prey of whales, would grow significantly as a consequence and exploratory krill fishing was practiced in some areas. However, it was found that there has been a substantial decline in abundance of krill since the end of whaling, which is the phenomenon of *krill paradox*. In this paper, to study the krill–whale interaction we revisit a harvested predator–prey model with Holling I functional response. We find that the model admits at most two positive equilibria. When the two positive equilibria are located in the region $\{(N, P)|0 \leq N < 2N_c,\ P \geq 0\}$, the model exhibits degenerate Bogdanov–Takens bifurcation with codimension up to 3 and Hopf bifurcation with codimension up to 2 by rigorous bifurcation analysis. When the two positive equilibria are located in the region $\{(N, P)|N > 2N_c,\ P \geq 0\}$, the model has no complex bifurcation phenomenon. When there is one positive equilibrium on each side of $N = 2N_c$, the model undergoes Hopf bifurcation with codimension up to 2. Moreover, numerical simulation reveals that the model not only can exhibit the krill paradox phenomenon but also

✉ Min Lu
lumin@mails.ccnu.edu.cn

Qin Pan
1364796996@qq.com

Jicai Huang
hjc@mail.ccnu.edu.cn

Shigui Ruan
ruan@math.miami.edu

[1] School of Mathematics and Statistics, and Key Lab NAA-MOE, Central China Normal University, Wuhan 430079, China

[2] Department of Mathematics, University of Miami, Coral Gables, FL 33146, USA

has three limit cycles, with the outmost one crosses the line $N = 2N_c$ under some specific parameter conditions.

Keywords Krill–whale interaction · Predator–prey model · Holling I functional response · Harvesting · Bogdanov–Takens bifurcation · Hopf bifurcation

Mathematics Subject Classification 34D05 · 34C23 · 34D25 · 92D25

1 Introduction

The Antarctic is a region where the largest human-induced perturbation of the marine ecosystem in the world has taken place (Mori and Butterworth 2004). Many species were harvested sequentially, with some species including whales heavily depleted as a consequence. Fearing that the whale stocks of the Antarctic would be depleted, in 1974 the International Union for the Conservation of Nature and Natural Resources adopted a set of "new management procedures", which divide the world's oceans into several areas, in each of which individual whale stocks are classified into one of three categories: If the stock is estimated to be 10% below the level where its potential yield is at the maximum sustainable yield (MSY), no harvesting is allowed; the whales are classified as "protection stock." If the stock is near the MSY level, annual quotas are set to keep the stock near that level; the whales are classified as "sustained management stock." If the estimated size of a stock is significantly above the MSY level, exploitation is allowed under quotas aimed at achieving a controlled reduction to that level; the whales are classified as "initial management stock" (Beddington and May 1982). In 1986, the depletion of whale populations by excessive harvesting over the years led the International Whaling Commission to forbid commercial whaling altogether (Mori and Butterworth 2006).

After reviewing the feeding of baleen whales in the Antarctic, Kawamura (1994) concluded that although there are some local and seasonal variations, all southern baleen whale species largely fulfill their nutritional requirements by feeding on krill, a key species within the Southern Ocean ecosystem. The overexploitation and decline of Southern Ocean stocks of krill-eating whales led to the *Krill Surplus Hypothesis* in the 1960s, which assumed that there were tens of thousands to more than a million tonnes of krill previously consumed by whales that could be taken for commercial purposes. Consequently the former Soviet Union and Japan initiated exploratory krill fishing in the Antarctic in the 1960s. However, late study found that there has been a substantial decline in abundance of krill since the end of whaling, this is the so-called *krill paradox* (Willis 2007, 2014; Savoca et al. 2021, Fig. 1a). To regulate krill fishery, the Convention for the Conservation of Antarctic Marine Living Resources (CCAMLR) was signed and entered into force in 1982 (Hofman 2017).

Various models have been proposed to describe the interactions between krill and whales with harvesting, see some early studies of May (1973), Beddington and May (1980), Horwood (1981), Yamanaka (1983), Butterworth and Thomson (1995), Mori and Butterworth (2004, 2006), etc. We refer to a review by Hill et al. (2006) on such models. May (1973) constructed a simple predator–prey model in which they

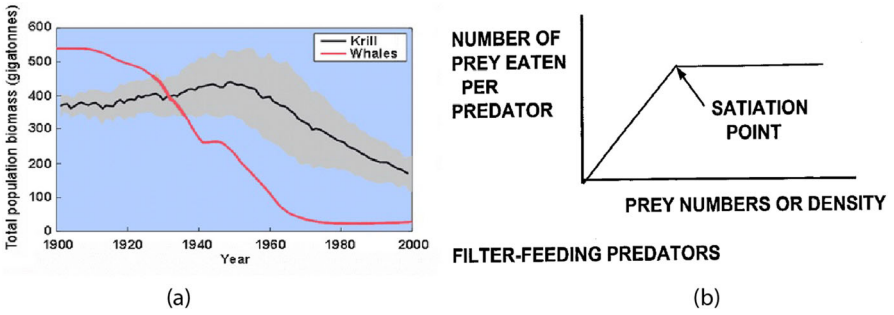

Fig. 1 **a** Krill paradox: The millions of whales killed due to commercial whaling resulted in a substantial decline in krill abundance (Willis 2014). **b** Holling Type I functional response: When prey abundance increases and reaches a critical value, the filter is filled and predation stops (Holling 1959)

assumed logistic growth in individual populations, with predation subtracted from the prey (krill) population, and the carrying capacity for the predator (whale) population determined by the abundance of its prey. They used a linear (Lotka-Volterra type) functional response to describe prey consumption per predator and demonstrated the potential impact of harvesting one species on other species.

Recall that Holling (1959) proposed three types of functional response based on different field data on different species. In particular, he proposed Type I functional response for a filter feeding predator, e.g. a baleen whale. As prey abundance increases, the swimming of the whale through the higher density of krill increases the number of prey eaten in direct proportion to prey abundance. However, at some abundance of prey, the filter is filled, and more prey cannot be taken (Fig. 1b).

In view of the impact of human activities on populations, it is necessary to uphold the principles of rational use of biological resources and sustainable development. Therefore, the predator–prey models with harvesting rates were developed to investigate the effects of harvesting on predator–prey interactions. Common types of harvesting are *constant-effort harvesting* and *constant-yield harvesting*, which were proposed by May et al. (1979), described by a constant multiplication of the size of the population under harvest and a constant independent of the size of the population under harvest, respectively. Additionally, *seasonal harvesting*, described by a periodic function, was considered in Chen et al. (2013). We refer to Brauer and Soudack (1979, 1981), Chen et al. (2013), Huang et al. (2016, 2013), Ruan and Xiao (2023), Xiao and Ruan (1999), and the references cited therein for stability and bifurcation analysis on predator–prey models with harvesting.

Following May (1973) and Holling (1959), we use a predator–prey model with Holling type I function response and constant-yield harvesting on both species to describe the interactions between krill and whales. Consider the following predator–prey system

$$\begin{aligned} \frac{dN}{d\tau} &= rN(1-\frac{N}{K}) - p(N)P - h_1, \\ \frac{dP}{d\tau} &= P[-\tilde{d} + \tilde{c}p(N)] - h_2, \end{aligned} \tag{1.1}$$

Table 1 Definitions of variables and parameters in system (1.1)

Variables or parameters (unit)	Description
$N(\tau)$ (numbers)	Density of prey (krill) at time τ (year)
$P(\tau)$ (numbers)	Density of predators (whales) at time τ (year)
r (1/year)	Intrinsic growth rate of prey
K (numbers)	Carrying capacity of prey
N_c (numbers)	Half-saturation constant (the number of prey at which the per capita predation rate is half of its maximum)
$\tilde{b}$ (1/year)	Maximum predation rate per predator
$\tilde{c}$ (none)	Conversion rate of predators
$\tilde{d}$ (1/year)	Mortality rate of predators
h_1 (numbers/year)	Harvest rate of prey
h_2 (numbers/year)	Harvest rate of predators

where $p(N)$ has the form

$$p(N) = \begin{cases} \frac{\tilde{b}}{2N_c} N, & 0 \le N \le 2N_c, \\ \tilde{b}, & N > 2N_c, \end{cases}$$

and the variables and parameters are listed in Table 1. Unlike the others, Holling type I functional response does not show a gradual saturation as the prey density increases, but instead flattens out abruptly when the prey density reaches a threshold value. Seo and DeAngelis (2011) gave a reasonable explanation of the "abrupt flatten out" phenomenon, which describes individual predators stop increasing their feeding rates when the prey density exceeds a threshold value (predators will find it easy to capture and assimilate prey, but will return to other activities once their ingestion rates are large enough to satisfy their needs).

Notice that system (1.1) is the same model proposed by Dai and Tang (1998). For the case $h_1 = h_2 = 0$ of model (1.1), Dubois and Closset (1975) observed the existence of two limit cycles numerically. Later, Ren and Han (1989) proved analytically the existence of at least two limit cycles. Moreover, Zegeling and Kooij (2020) considered system (1.1) with $h_1 = h_2 = 0$ and $\widetilde{c} = 1$, and showed that the maximum number of limit cycles is two. Dai and Xu (1994, 1991) considered the cases $h_1 = 0$ but $h_2 \neq 0$ and $h_1 \neq 0$ but $h_2 = 0$, respectively. They provided some vigorous proofs for the existence of multiple limit cycles. For the case $h_1 \neq 0$ and $h_2 \neq 0$, Dai and Tang (1998) found that the maximum safe harvest may be far less than what would be assumed from a local analysis for the equilibria. Moreover, the numbers and types of equilibria of model (1.1) were given. System (1.1) has at most two positive equilibria, however, they especially studied the case when system (1.1) has one equilibrium point on each side of $N = 2N_c$, and proved that model (1.1) can exhibit complex dynamics such as the existence of multiple limit cycles and homoclinic orbits by using qualitative analysis and Poincaré-Bendixson theorem.

The purpose of this paper is to study model (1.1) with constant-yield harvesting in both prey and predators and Holling type I functional response. Note that $p(N)$ is a piecewise-continuous function which is linear when $N \leq 2N_c$ and constant when $N > 2N_c$, so that model (1.1) has linear predation when $N \leq 2N_c$ and constant predation when $N > 2N_c$, but is singular at $N = 2N_c$. We will show that model (1.1) has different dynamics in these three cases and combine them to obtain the dynamics for the whole system. (i) When there are two positive equilibria in the region $\{(N, P)|0 \leq N < 2N_c,\ P \geq 0\}$, we find that model (1.1) exhibits degenerate Bogdanov–Takens bifurcation with codimension up to 3 and Hopf bifurcation with codimension up to 2 by rigorous bifurcation analysis. (ii) When two positive equilibria are located in the region $\{(N, P)|N > 2N_c,\ P \geq 0\}$, model (1.1) has no complex bifurcation phenomenon since one positive equilibrium is always a saddle and the other is always an unstable node. (iii) When there is one positive equilibrium on each side of $N = 2N_c$, system (1.1) undergoes Hopf bifurcation with codimension up to 2 around the left positive equilibrium. Moreover, numerical simulation reveals that system (1.1) has three limit cycles with the outmost one crosses the line $N = 2N_c$ under some specific parameter conditions.

Before going into details, we firstly rescale system (1.1) by introducing

$$N = Kx, \quad P = \tilde{c}Ky, \quad \tau = \frac{2N_c}{\tilde{c}\tilde{b}K}t,$$

then system (1.1) becomes

$$\begin{aligned} \frac{dx}{dt} &= ax(1-x) - T(x)y - b, \\ \frac{dy}{dt} &= y[T(x) - c] - d, \end{aligned} \tag{1.2}$$

where

$$a = \frac{2rN_c}{\tilde{b}\tilde{c}K},\ b = \frac{2h_1N_c}{\tilde{b}\tilde{c}K^2},\ c = \frac{2\tilde{d}N_c}{\tilde{b}\tilde{c}K},\ d = \frac{2h_2N_c}{\tilde{b}\tilde{c}^2K^2},\ n = \frac{2N_c}{K},$$
$$T(x) = \frac{n + x - |x - n|}{2},$$

and $a,\ b,\ c,\ d,\ n > 0$. Obviously, the first quadrant is no longer positively invariant under the flow of system (1.2), which makes the theoretical analysis more challenge. From the standpoint of biology, we are only interested in the dynamics of system (1.2) in the first quadrant.

When $x < n$, system (1.2) becomes

$$\begin{aligned} \frac{dx}{dt} &= ax(1-x) - xy - b, \\ \frac{dy}{dt} &= y(x - c) - d, \end{aligned} \tag{1.3}$$

which is called the *left system*, the feasible region of system (1.3) is

$$D_1 = \{(x, y)|0 \le x < n,\ y \ge 0\}.$$

When $x > n$, system (1.2) becomes

$$\begin{aligned} \frac{dx}{dt} &= ax(1-x) - ny - b, \\ \frac{dy}{dt} &= y(n-c) - d, \end{aligned} \tag{1.4}$$

which is called the *right system*, the feasible region of system (1.4) is

$$D_2 = \{(x, y)|x > n,\ y \ge 0\}.$$

The rest of the paper is organized as follows. In Sects. 2–4, we carry out a qualitative analysis to give the types and stabilities of equilibria of system (1.3), (1.4) and the full system (1.2), respectively. In Sect. 5, we investigate the dynamics and bifurcations of system (1.2). In Sect. 6, we give some portraits of the full system (1.2). We summarize the results and suggest future research topics in the last section.

2 Equilibria and types of the left system (1.3)

If $E(x^*, y^*)$ is an equilibrium of system (1.3) in D_1, then $y^* = \frac{d}{x^*-c}$ and $x^* \in I_1$ is a real root of $f(x) = 0$, where

$$I_1 := \{x \in \mathbb{R} : c < x < \min\{1, n\}\},\ f(x) := ax^3 - a(1+c)x^2 + (b + ac + d)x - bc. \tag{2.1}$$

First of all, we notice that

$$\lim_{x\to-\infty} f(x) = -\infty, \quad \lim_{x\to+\infty} f(x) = +\infty, \quad f(c) = cd > 0, \tag{2.2}$$

and

$$f'(x) = 3ax^2 - 2a(1+c)x + b + ac + d. \tag{2.3}$$

The discriminant of $f'(x) = 0$ is $\tilde{\Delta} := 4a^2(1+c)^2 - 12a(b + ac + d)$, and

$$\tilde{\Delta} \le 0 \Longleftrightarrow a \le \frac{3(b+d)}{c^2 - c + 1}.$$

Thus, if $a \le \frac{3(b+d)}{c^2-c+1}$, then $f'(x) \ge 0$ for any $x \in R$, and $f(x)$ has no real root in I_1; i.e., system (1.3) has no positive equilibrium in D_1. If $a > \frac{3(b+d)}{c^2-c+1}$, i.e., $\tilde{\Delta} > 0$, then

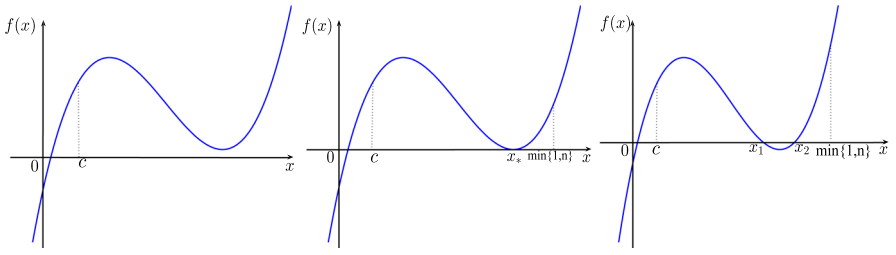

Fig. 2 The real roots in I_1 of $f(x) = 0$ when $a > \frac{3(b+d)}{c^2-c+1}$: **a** no positive root; **b** a double positive root x_* $(= \overline{x}_2)$; **c** two single positive roots x_1 and x_2

$f'(x) = 0$ has the following two real roots:

$$\overline{x}_1 = \frac{-\sqrt{\tilde{\Delta}} + a(1+c)}{3a} > 0, \quad \overline{x}_2 = \frac{\sqrt{\tilde{\Delta}} + a(1+c)}{3a} > 0. \tag{2.4}$$

Combining these and the property (2.2), we are able to plot the possible curves of $f(x)$ (see Fig. 2). From Fig. 2a–c, we can see that when $a > \frac{3(b+d)}{c^2-c+1}$, $f(x) = 0$ can have zero positive root, or one double positive root x_* $(= \overline{x}_2)$, or two single positive roots x_1 and x_2 in I_1, respectively. Accordingly, system (1.3) can have zero, one (E_*), or two positive equilibria (E_1, E_2) in D_1.

We further discuss the stability of positive equilibria. The Jacobian matrix of system (1.3) at any equilibrium $E(x^*, y^*)$ is

$$J(E) = \begin{pmatrix} -2ax^* + a + \frac{d}{c-x^*} & -x^* \\ \frac{d}{x^*-c} & x^* - c \end{pmatrix}.$$

From $f(x^*) = 0$, we have

$$b = \frac{x^*\big(d - a(x^*-1)(c-x^*)\big)}{c-x^*}, \tag{2.5}$$

then

$$\mathrm{Det}(J(E)) = \frac{a(2x^*-1)(c-x^*)^2 - cd}{c-x^*} = -f'(x^*), \tag{2.6}$$

$$\mathrm{Tr}(J(E)) = \frac{(c-x^*)(2ax^* - a + c - x^*) - d}{x^*-c}. \tag{2.7}$$

It implies that $E(x^*, y^*)$ is a hyperbolic saddle if $f'(x^*) > 0$, an elementary equilibrium if $f'(x^*) \neq 0$, and a degenerate equilibrium if $f'(x^*) = 0$. We have the following results.

Lemma 2.1 *Let $f(x)$, I_1 and $\overline{x}_2$ be given by (2.1) and (2.4), respectively. System (1.3) has no boundary equilibrium, and at most two positive equilibria in D_1. The possible cases are included in Table 2.*

Proof For $n \leq c$, from the second equation of system (1.3), we can get $\frac{dy}{dt} = y(x - c) - d < 0$ if $x < n \leq c$, which implies that system (1.3) has no equilibrium in D_1 if $n \leq c$.

For $n > c$, we consider three cases as follows: **Case (I)**: $n > c$, $f(n) > 0$, **Case (II)**: $n > c$, $f(n) < 0$ and **Case (III)**: $n > c$, $f(n) = 0$.

Case (I)(i): $n > c$, $f(n) > 0$ and $n \leq \frac{1}{2}$. From the property of $f(x)$ and $f'(x)$, we see that if $f(n) > 0$, there are three possible cases for the distribution of the roots of $f(x) = 0$ in I_1: (a) $f(x) = 0$ has no real root in I_1; (b) $f(x) = 0$ has a double root x_* in I_1; (c) $f(x) = 0$ has two different roots x_1 and x_2 in I_1. But under the condition $n \leq \frac{1}{2}$, we can see that the cases (b) and (c) do not exist. In fact, since $f(0) = -bc < 0$ and $f(c) > 0$, then there exists $\bar{x}_0 \in (0, c)$ such that $f(\bar{x}_0) = 0$. By the vieta's theorem, we know that $\bar{x}_0 + 2x_* = 1 + c$ for the case (b), i.e., $2x_* = 1 + c - \bar{x}_0 > 1$, thus $x_* > \frac{1}{2}$. However $x_* < n \leq \frac{1}{2}$, which is a contradiction. For the case (c), we have $\bar{x}_0 + x_1 + x_2 = 1 + c$, i.e., $x_1 + x_2 = 1 + c - \bar{x}_0 > 1$. On the other hand, since $x_1 < n \leq \frac{1}{2}$ and $x_2 < n \leq \frac{1}{2}$, then $x_1 + x_2 < 1$, which is also a contradiction. Hence, if $n > c$, $f(n) > 0$ and $n \leq \frac{1}{2}$, then $f(x) = 0$ has no real root in I_1. **Case (I)(ii)**: $n > c$, $f(n) > 0$ and $n > \frac{1}{2}$. From the property of $f(x)$, when $a \leq \frac{3(b+d)}{c^2-c+1}$, then $f(x) = 0$ has no real root in I_1. When $a > \frac{3(b+d)}{c^2-c+1}$, $f(x) = 0$ can have zero, one, or two positive real roots in I_1.

Case (II): When $n > c$ and $f(n) < 0$, then $x_1 < n < x_2$. Thus, if $x_1 \in I_1$, then $E_1(x_1, y_1)$ is an equilibrium of system (1.3) in D_1, where $y_1 = \frac{d}{x_1 - c}$.

Case (III): From the above analyses, we have the following facts: if x_1 and x_2 are the different roots of $f(x)$ in I_1, then $x_1 + x_2 > 1$; if x_* is a double root of $f(x)$ in I_1, then $x_* > \frac{1}{2}$. Since $f(n) = 0$, we have $n = x_1$, or $n = x_2$, or $n = x_*$. **Case (III)(i)**: $n > c$, $f(n) = 0$ and $n \leq \frac{1}{2}$. Obviously, if $x_1 = n$, then $x_1 \notin I_1$; if $x_* = n$, then $x_* \leq \frac{1}{2}$, which is a contradiction; if $x_2 = n$, for $x_1 < x_2$, we can get $x_1 + x_2 < 2n \leq 1$, which is also a contradiction. Thus, system (1.3) has no equilibrium in this case. **Case (III)(ii)**: $n > c$, $f(n) = 0$ and $n > \frac{1}{2}$. From the above discussion, in this case system (1.3) has a unique equilibrium E_1 if and only if $x_2 = n$ and $x_1 \in I_1$. □

We next consider the detailed types of the double equilibrium $E_*(x_*, y_*)$, where x_* is the double positive root of $f(x) = 0$ in I_1. From $f(x_*)$=$f'(x_*)$=0, a and b can be expressed by c, d and x_* as

$$\begin{aligned} a = a_0 &:= \frac{cd}{(2x_* - 1)(c - x_*)^2}, \\ b = b_0 &:= \frac{dx_*^2(c - 2x_* + 1)}{(2x_* - 1)(c - x_*)^2}. \end{aligned} \tag{2.8}$$

Table 2 Numbers of equilibria in the left system (1.3) (see Lemma 2.1 for proof)

$n-c$	$f(n)$	$n-\frac{1}{2}$	$a-\frac{3(b+d)}{c^2-c+1}$	$f(\bar{x}_2)$	x_*, x_1, x_2	Numbers	Equilibrium
≤ 0						0	
>0	>0	≤ 0				0	
		>0	≤ 0			0	
			>0	>0		0	
				$=0$	$x_* \notin I_1$	0	
					$x_* \in I_1$	1	E_* (degenerate)
				<0	$x_1 \in I_1, x_2 \in I_1$	2	E_1 (anti-saddle), E_2 (saddle)
					$x_1 \in I_1, x_2 \notin I_1$	1	E_1 (anti-saddle)
					$x_1 \notin I_1, x_2 \notin I_1$	0	
	<0				$x_1 \in I_1$	1	E_1 (anti-saddle)
					$x_1 \notin I_1$	0	
	$=0$	≤ 0			$x_1 = n$	0	
		>0			$x_1 = n$ or $x_* = n$	0	
					$x_2 = n, x_1 \in I_1$	1	E_1 (anti-saddle)
					$x_2 = n, x_1 \notin I_1$	0	

From $a_0 > 0$, $b_0 > 0$ and $x_* \in I_1$, we have $0 < c < 1$ and $x_* \in I_2$, where

$$I_2 := \left\{ x_* \in \mathbb{R} : \max\left\{c, \frac{1}{2}\right\} < x_* < \min\left\{n, \frac{1+c}{2}\right\}\right\}.$$

Moreover, from $\mathrm{Tr}(J(E_*))=0$ and (2.8), d can be expressed by c and x_* as

$$d = d_0 := -\frac{(c-x_*)^3}{x_*}. \tag{2.9}$$

Let

$$\begin{aligned} \bar{c}_1 &= \frac{1}{4}\left(4x_* - 1 - \sqrt{-16x_*^2 + 8x_* + 1}\right), \\ \bar{c}_2 &= \frac{1}{4}\left(4x_* - 1 + \sqrt{-16x_*^2 + 8x_* + 1}\right). \end{aligned} \tag{2.10}$$

Then, we have the types of E_* as follows.

Theorem 2.2 *If $0 < c < 1$, $x_* \in I_2$ and the conditions in (2.8) are satisfied, then system (1.3) has a unique positive equilibrium $E_*(x_*, y_*)$, which is degenerate. Moreover,*

(I) *if $d \neq d_0$, then E_* is a saddle-node with a stable (or unstable) parabolic sector if $d > d_0$ (or $d < d_0$);*
(II) *if $d = d_0$, then E_* is a cusp. Furthermore,*

(i) $E_*(x_*, y_*)$ *is a cusp of codimension 2 if one of the following conditions is satisfied:*
(i1) $x_* > \frac{1}{4}(1+\sqrt{2})$;
(i2) $x_* < \frac{1}{4}(1+\sqrt{2})$, $c \neq \bar{c}_1$ *and* $c \neq \bar{c}_2$;
(i3) $x_* = \frac{1}{4}\left(1+\sqrt{2}\right)$ *and* $c \neq \frac{1}{2\sqrt{2}}$;

(ii) $E_*(x_*, y_*)$ *is a cusp of codimension 3 if one of the following conditions is satisfied:*
(ii1) $x_* < \frac{1}{4}\left(1+\sqrt{2}\right)$, $c = \bar{c}_1$ *or* $c = \bar{c}_2$;
(ii2) $x_* = \frac{1}{4}\left(1+\sqrt{2}\right)$ *and* $c = \frac{1}{2\sqrt{2}}$.

Proof We first transform E_* into the origin by letting $X = x - x_*$, $Y = y - y_*$ (still denote X, Y by x, y, respectively):

$$\begin{aligned} \frac{dx}{dt} &= -\frac{dx_*}{(c-x_*)^2}x - x_*y - \frac{cd}{(2x_*-1)(c-x_*)^2}x^2 - xy + o(|x,y|^2), \\ \frac{dy}{dt} &= \frac{d}{x_*-c}x + (x_*-c)y + xy + o(|x,y|^2), \end{aligned} \tag{2.11}$$

where a and b are eliminated by $a = a_0$ and $b = b_0$, respectively.

Case (I): $d \neq d_0$. Let $x = -\frac{(c-x_*)^2}{d}X + \frac{x_*}{c-x_*}Y$, $y = X + Y$ and $\tau = (-\frac{dx_*}{(c-x_*)^2} - c + x_*)t$, then system (2.11) becomes (still denote X, Y, τ by x, y, t, respectively)

$$\begin{aligned} \frac{dx}{dt} &= a_1x^2 + a_2xy + a_3y^2 + o(|x,y|^2), \\ \frac{dy}{dt} &= y + b_1x^2 + b_2xy + b_3y^2 + o(|x,y|^2), \end{aligned} \tag{2.12}$$

where

$$a_1 = -\frac{c(c-3x_*+1)(c-x_*)^4}{(2x_*-1)\left((c-x_*)^3 + dx_*\right)^2}, \tag{2.13}$$

to save space, we omit the expressions for a_2, a_3, b_1, b_2 and b_3 here. Notice that $a_1 > 0$, then according to Theorem 7.1 in Zhang et al. (1992), the equilibrium (x_*, y_*) is a saddle-node, which includes an unstable (a stable) parabolic sector if $d < d_0$ ($d > d_0$).

Case (II): $d = d_0$. Let $x = \frac{x_*}{c-x_*}X$, $y = X - \frac{1}{c-x_*}Y$, then system (2.11) can be rewritten as (still denote X, Y by x, y, respectively)

$$\begin{aligned} \frac{dx}{dt} &= y + \frac{c-2x_*+1}{2x_*-1}x^2 + \frac{1}{c-x_*}xy + o(|x,y|^2), \\ \frac{dy}{dt} &= \frac{c(c-3x_*+1)}{2x_*-1}x^2 + \frac{c}{c-x_*}xy + o(|x,y|^2). \end{aligned} \tag{2.14}$$

By Remark 1 of section 2.13 in Perko (2001) (see also Lemma 3.1 in Huang et al. 2013), we obtain an equivalent system of (2.14) in the small neighborhood of (0, 0) as follows:

$$\begin{aligned} \frac{dx}{dt} &= y, \\ \frac{dy}{dt} &= Dx^2 + Exy + o(|x, y|^2), \end{aligned} \tag{2.15}$$

where

$$D = \frac{c\,(c - 3x_* + 1)}{2x_* - 1}, \quad E = \frac{2c^2 + c\,(1 - 4x_*) + 2x_*\,(2x_* - 1)}{(2x_* - 1)\,(c - x_*)}. \tag{2.16}$$

It is easy to see that $D < 0$ and the sign of the denominator of E is negative, since $x_* > \max\{c, \frac{1}{2}\}$. If $x_* > \frac{1}{4}\left(1 + \sqrt{2}\right)$, or $x_* < \frac{1}{4}\left(1 + \sqrt{2}\right)$, $c \neq \bar{c}_1$ and $c \neq \bar{c}_2$, or $x_* = \frac{1}{4}\left(1 + \sqrt{2}\right)$ and $c \neq \frac{1}{2\sqrt{2}}$, then $E \neq 0$. Thus we have the conclusions of case (II)(i).

Case (II)(ii): We can use several steps to convert system (1.2) into its equivalent system [see Theorem 2.7 in Xiang et al. (2020), or Lemma 2.4 in Lu et al. (2023), or Theorem 1 in Zhang et al. (2023)]:

$$\begin{aligned} \frac{d\widetilde{X}_4}{dt} &= \widetilde{Y}_4, \\ \frac{d\widetilde{Y}_4}{dt} &= \widetilde{X}_4^2 + M_i \widetilde{X}_4^3 \widetilde{Y}_4 + o(|\widetilde{X}_4, \widetilde{Y}_4|^4), \end{aligned} \tag{2.17}$$

where $i = 1$, $i = 2$ and $i = 3$ corresponding the cases $c = \bar{c}_1$, $c = \bar{c}_2$ and $c = \frac{1}{2\sqrt{2}}$, respectively. Moreover,

$$\begin{aligned} M_1 &= \frac{2[w_1 - (16x_*^2 - 4x_* - 1)]}{\{x_*\big(w_1\,(6x_* - 1) + 8x_*^2 + 2x_* - 1\big)\}^{\frac{3}{2}}} < 0, \\ M_2 &= \frac{2\big(-w_1 - (16x_*^2 - 4x_* - 1)\big)}{\{x_*\big(w_1(1 - 6x_*) + 8x_*^2 + 2x_* - 1\big)\}^{\frac{3}{2}}} < 0, \\ M_3 &= -\frac{16}{7}\sqrt{\frac{1}{7}\left(296 - 206\sqrt{2}\right)} < 0, \end{aligned}$$

where

$$w_1 = \sqrt{-16x_* + 8x_* + 1} > 0.$$

In fact, since $\frac{1}{2} < x_* < \frac{1}{4}\left(1+\sqrt{2}\right)$, then $6x_* - 1 > 0$, $8x_*^2 + 2x_* - 1 > 0$ and $16x_*^2 - 4x_* - 1 > 0$. Since

$$w_1^2 - (16x_*^2 - 4x_* - 1)^2 = 128\,(1-2x_*)\,x_*^3 < 0$$

and

$$(8x_*^2 + 2x_* - 1)^2 - \left(w_1(1-6x_*)\right)^2 = 64x_*^2\left(10x_*^2 - 7x_* + 1\right) > 0,$$

then $w_1 - (16x_*^2 - 4x_* - 1) < 0$ and $w_1(1-6x_*) + 8x_*^2 + 2x_* - 1 > 0$. Therefore, $M_1 < 0$ and $M_2 < 0$. Thus, E_* is a cusp of codimension 3 (Dumortier et al. 1987).

Therefore, we complete the proof. □

Next we discuss the types of the single equilibria $E_1(x_1, y_1)$ and $E_2(x_2, y_2)$. Let

$$d^H := (c - x_1)\left(a\,(2x_1 - 1) + c - x_1\right). \tag{2.18}$$

Theorem 2.3 *If equilibria E_1 and E_2 exist, then $E_2(x_2, y_2)$ is always a hyperbolic saddle, and*

(I) *$E_1(x_1, y_1)$ is a hyperbolic unstable node or focus if $d < d^H$ and $c < x_1 \le \frac{1}{2}$, or $d < d^H$, $x_1 > \max\{c, \frac{1}{2}\}$ and $a < \frac{c-x_1}{1-2x_1}$;*

(II) *$E_1(x_1, y_1)$ is a hyperbolic stable node or focus if $d > d^H$;*

(III) *$E_1(x_1, y_1)$ is a weak focus or center if $d = d^H$ and $c < x_1 \le \frac{1}{2}$, or $d = d^H$, $x_1 > \max\{c, \frac{1}{2}\}$ and $a < \frac{c-x_1}{1-2x_1}$.*

Proof The conditions $c < x_1 \le \frac{1}{2}$, or $x_1 > \max\{c, \frac{1}{2}\}$ and $a < \frac{c-x_1}{1-2x_1}$ guarantee $d^H > 0$. From (2.7), it is easy to see that $\mathrm{Tr}(J(E_1)) > 0$, $\mathrm{Tr}(J(E_1)) = 0$ and $\mathrm{Tr}(J(E_1)) < 0$ if $d < d^H$, $d = d^H$ and $d > d^H$, respectively, leading to the conclusions. □

3 Equilibria and types of the right system (1.4)

If $\widetilde{E}(\widetilde{x}, \widetilde{y})$ is an equilibrium of system (1.4) in D_2, then $\widetilde{y} = \frac{d}{n-c}$ and $\widetilde{x} \in I_3$ is a real root of $\widetilde{f}(x) = 0$, where $n > c$ and

$$I_3 := \{x \in \mathbb{R} : n < x < 1\}, \quad \widetilde{f}(x) := a(n-c)x^2 + a(c-n)x + dn + b(n-c). \tag{3.1}$$

We further discuss the stability of possible equilibria. The Jacobian matrix of system (1.4) at any equilibrium $\widetilde{E}(\widetilde{x}, \widetilde{y})$ is

$$J(\widetilde{E}) = \begin{pmatrix} a(1-2\widetilde{x}) & -n \\ 0 & n-c \end{pmatrix}.$$

From $\widetilde{f}(\widetilde{x}) = 0$, we have

$$d = \frac{(c-n)(a(\widetilde{x}-1)\widetilde{x}+b)}{n}, \tag{3.2}$$

then

$$\mathrm{Det}(J(\widetilde{E})) = a(2\widetilde{x}-1)(c-n), \quad \mathrm{Tr}(J(\widetilde{E})) = a(1-2\widetilde{x})+n-c. \tag{3.3}$$

It implies that $E(\widetilde{x},\widetilde{y})$ is a hyperbolic saddle if $\widetilde{x} > \frac{1}{2}$, an elementary equilibrium if $\widetilde{x} \neq \frac{1}{2}$, and a degenerate equilibrium if $\widetilde{x} = \frac{1}{2}$. We have the following results.

Lemma 3.1 *System (1.4) in D_2 has no boundary equilibrium and at most two positive equilibria $\widetilde{E}_1$ and $\widetilde{E}_2$, which can coalesce into a unique positive equilibrium $\widetilde{E}_*$ (see Table 3 for detailed classifications).*

Proof Obviously, we have $\widetilde{f}(n) = f(n)$.

When $n \le c$, from the second equation of system (1.4), we obtain $\frac{dy}{dt} = y(n-c) - d < 0$, which implies that system (1.4) has no equilibrium if $n \le c$.

When $n > c$, we have $\widetilde{f}(1) = dn + b(n-c) > 0$ and consider three cases as follows: **case (I)**: $n > c$ and $f(n) > 0$, **case (II)**: $n > c$ and $f(n) < 0$, **case (III)**: $n > c$ and $f(n) = 0$.

Case (I)(i): $n > c$, $f(n) > 0$ and $n < \frac{1}{2}$. The discriminant of $\widetilde{f}(x) = 0$ is

$$\Delta = a(c-n)[a(c-n) - 4bc + 4bn + 4dn]. \tag{3.4}$$

When $a < \frac{4(bc-bn-dn)}{c-n}$, i.e., $\Delta < 0$, then $\widetilde{f}(x) = 0$ has no real root; when $a = \frac{4(bc-bn-dn)}{c-n}$, then $\widetilde{f}(x) = 0$ has a double root $\widetilde{x}_* = \frac{1}{2} \in I_3$; when $a > \frac{4(bc-bn-dn)}{c-n}$, i.e., $\Delta > 0$, then $\widetilde{f}(x) = 0$ has two real roots $\widetilde{x}_1$ and $\widetilde{x}_2$, where $\widetilde{x}_1 < \frac{1}{2} < \widetilde{x}_2$. Since $f(n) > 0$ ($n < \frac{1}{2}$) and $\widetilde{f}(1) > 0$, we know that $\widetilde{x}_1 \in I_3$ and $\widetilde{x}_2 \in I_3$. **Case (I)(ii)**: $n > c$, $f(n) > 0$ and $n \ge \frac{1}{2}$. In this case, we have $\widetilde{f}(x) > 0$ when $n < x < 1$. Thus $\widetilde{f}(x) = 0$ has no real root in I_3, i.e., system (1.4) has no equilibrium in D_2.

Case (II): $n > c$ and $f(n) < 0$. In this case, we have $\widetilde{x}_1 < n < \widetilde{x}_2 < 1$, then $\widetilde{x}_1 \notin I_3$ and $\widetilde{x}_2 \in I_3$.

Case (III): $n > c$ and $f(n) = 0$. In this case, we have $n = \widetilde{x}_1$, or $n = \widetilde{x}_*$, or $n = \widetilde{x}_2$. Since $\widetilde{x}_1 < \widetilde{x}_* = \frac{1}{2} < \widetilde{x}_2$, we have $\widetilde{x}_1 = n$, $\widetilde{x}_* = n$ and $\widetilde{x}_2 = n$ if $n < \frac{1}{2}$, $n = \frac{1}{2}$ and $n > \frac{1}{2}$, respectively. When $\widetilde{x}_1 = n$, we can get $\widetilde{x}_2 \in I_3$ for $\widetilde{f}(1) > 0$. □

Theorem 3.2 *$\widetilde{E}_1(\widetilde{x}_1,\widetilde{y}_1)$ is always an unstable node and $\widetilde{E}_2(\widetilde{x}_2,\widetilde{y}_2)$ is always a hyperbolic saddle if $\widetilde{E}_1$ and $\widetilde{E}_2$ exist. $\widetilde{E}_*(\widetilde{x}_*,\widetilde{y}_*)$ is a saddle-node if it exists.*

Proof If $\widetilde{E}_1$ and $\widetilde{E}_2$ exist, then $\widetilde{x}_1 < \frac{1}{2}$ and $n > c$. From (3.3), we have $\mathrm{Det}(J(\widetilde{E}_1)) > 0$ and $\mathrm{Tr}(\widetilde{E}_1)) > 0$. Moreover, $\mathrm{Tr}^2(\widetilde{E}_1) - 4\mathrm{Det}(J(\widetilde{E}_1)) > 0$, so $\widetilde{E}_1(\widetilde{x}_1,\widetilde{y}_1)$ is an unstable node. Furthermore, since $\widetilde{x}_2 > \frac{1}{2}$ and $n > c$, we have $\mathrm{Det}(J(\widetilde{E}_2)) < 0$, which means that $\widetilde{E}_2(\widetilde{x}_2,\widetilde{y}_2)$ is a hyperbolic saddle.

Table 3 Numbers of equilibria in the right system (1.4) (see Lemma 3.1 for proof)

$n-c$	$f(n)$	$n-\frac{1}{2}$	$a-\frac{4(bc-bn-dn)}{c-n}$	$\widetilde{x}_*, \widetilde{x}_1, \widetilde{x}_2$	Numbers	Equilibrium
≤ 0					0	
>0	>0	<0	<0		0	
			$=0$	$\widetilde{x}_*=\frac{1}{2}$	1	$\widetilde{E}_*$ (saddle-node)
			>0	$\widetilde{x}_1 \in I_3, \widetilde{x}_2 \in I_3$	2	$\widetilde{E}_1$ (unstable node), $\widetilde{E}_2$ (saddle)
		≥ 0			0	
	<0			$\widetilde{x}_2 \in I_3$	1	$\widetilde{E}_2$ (saddle)
	$=0$	<0		$\widetilde{x}_1=n, \widetilde{x}_2 \in I_3$	1	$\widetilde{E}_2$ (saddle)
		$=0$		$\widetilde{x}_*=n$	0	
		>0		$\widetilde{x}_2=n$	0	

Next, we discuss the type of $\widetilde{E}_*$. We transform $\widetilde{E}_*(\widetilde{x}_*, \widetilde{y}_*)$ into the origin by letting $X=x-\widetilde{x}_*$, $Y=y-\widetilde{y}_*$, where $\widetilde{x}_*=\frac{1}{2}$ and $\widetilde{y}_*=\frac{d}{n-c}$, and rewrite system (1.4) as follows (still denote X, Y by x, y, respectively):

$$\begin{aligned} \frac{dx}{dt} &= -ny - ax^2 + o(|x,y|^4), \\ \frac{dy}{dt} &= (n-c)y + o(|x,y|^4). \end{aligned} \tag{3.5}$$

Let $x=X+\frac{n}{c-n}Y$, $y=Y$ and $\tau=(n-c)t$, then system (3.5) becomes (still denote X, Y, τ by x, y, t, respectively)

$$\begin{aligned} \frac{dx}{dt} &= \frac{a}{c-n}x^2 + \frac{2an}{(c-n)^2}xy + \frac{an^2}{(c-n)^3}y^2 + o(|x,y|^4), \\ \frac{dy}{dt} &= y + o(|x,y|^4). \end{aligned} \tag{3.6}$$

Since $\frac{a}{c-n} < 0$, according to Theorem 7.1 in Zhang et al. (1992), the equilibrium $(\widetilde{x}_*, \widetilde{y}_*)$ is a saddle-node. □

4 Equilibria of the full system (1.2)

From Lemmas 2.1 and 3.1, we have the following theorem about the equilibria on the line $x=n$, where the response function undergoes an abrupt change.

Theorem 4.1 *When $n>c$ and $f(n)=0$, system (1.2) has an equilibrium E_n on the line $x=n$. More precisely,*

(I) *if $n<\frac{1}{2}$, then $x_1=\widetilde{x}_1=n$, i.e., E_1 and $\widetilde{E}_1$ coincide as E_n (see Fig. 3a);*
(II) *if $n=\frac{1}{2}$, then $x_1=\widetilde{x}_*=n$, i.e., E_1 and $\widetilde{E}_*$ coincide as E_n (see Fig. 3b);*
(III) *if $n>\frac{1}{2}$ and*

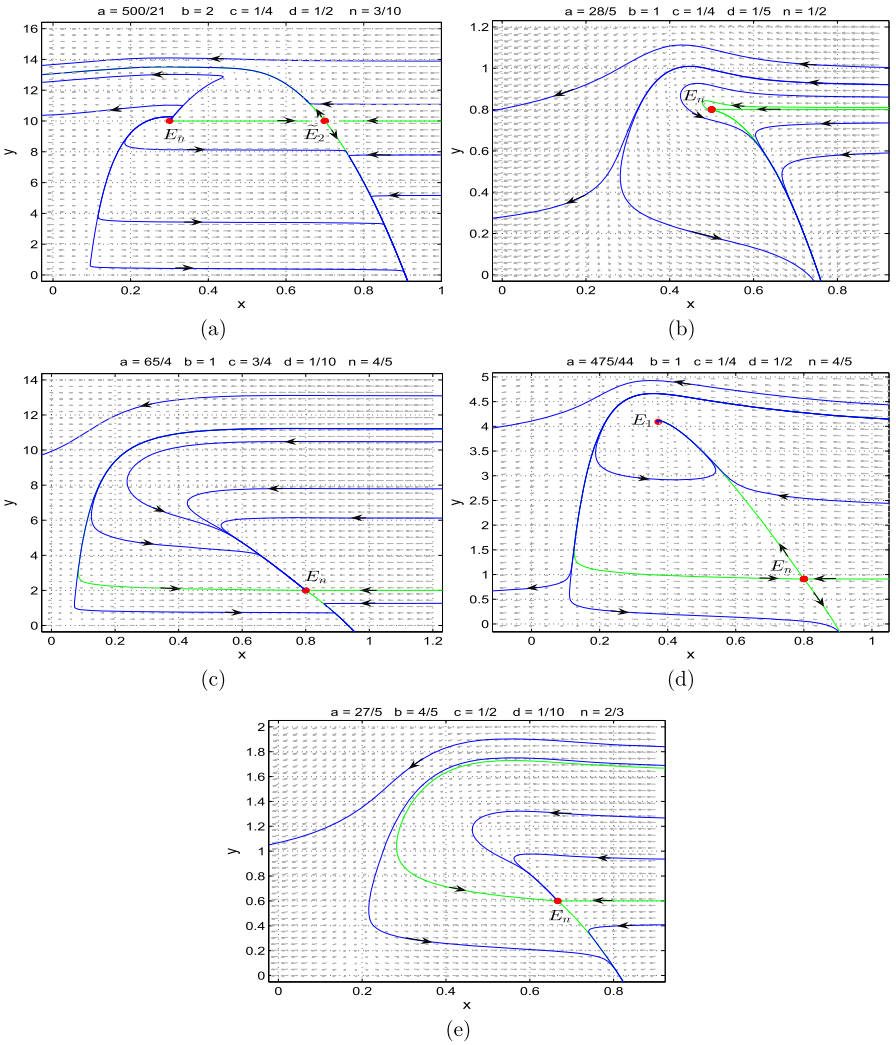

Fig. 3 Equilibria of the full system (1.2) with E_n located on the line $x = n$. **a** E_1 and $\widetilde{E}_1$ coincide as E_n, and $\widetilde{E}_2 \in D_2$; **b** E_1 and $\widetilde{E}_*$ coincide as E_n; **c** E_1 and $\widetilde{E}_2$ coincide as E_n; **d** E_2 and $\widetilde{E}_2$ coincide as E_n, and $E_1 \in D_1$; **e** E_* and $\widetilde{E}_2$ coincide as E_n

(i) $x_1 = \widetilde{x}_2 = n$, *then* E_1 *and* $\widetilde{E}_2$ *coincide as* E_n *(see Fig. 3c);*
(ii) $x_2 = \widetilde{x}_2 = n$, *then* E_2 *and* $\widetilde{E}_2$ *coincide as* E_n *(see Fig. 3d);*
(iii) $x_* = \widetilde{x}_2 = n$, *then* E_* *and* $\widetilde{E}_2$ *coincide as* E_n *(see Fig. 3e).*

3 Summarizing Tables 2, 3 and Lemma 4.1, we have the following theorem.

Theorem 4.2 *The full system* (1.2) *has no boundary equilibrium and at most two positive equilibria (see detailed classification in Table* 4*).*

Table 4 Numbers of equilibria in the full system (1.2)

$n-c$	$f(n)$	$n-\frac{1}{2}$	$a-\frac{3(b+d)}{c^2-c+1}$	$a-\frac{4(bc-bn-dn)}{c-n}$	$f(\bar{x}_2)$	x_*, x_1, x_2 $\widetilde{x}_*, \widetilde{x}_1, \widetilde{x}_2$	Numbers	Equilibrium
≤ 0							0	
>0	>0	>0	≤ 0				0	
			>0		>0		0	
					$=0$	$x_* \notin I_1$	0	
						$x_* \in I_1$	1	E_* (degenerate)
					<0	$x_1 \notin I_1, x_2 \notin I_1$	0	
						$x_1 \in I_1, x_2 \notin I_1$	1	E_1 (anti-saddle)
						$x_1 \in I_1, x_2 \in I_1$	2	E_1 (anti-saddle), E_2 (saddle)
		$=0$					0	
		<0		<0			0	
				$=0$		$\widetilde{x}_* = \frac{1}{2}$	1	$\widetilde{E}_*$ (saddle-node)
				>0		$\widetilde{x}_1 \in I_3, \widetilde{x}_2 \in I_3$	2	$\widetilde{E}_1$ (unstable node), $\widetilde{E}_2$ (saddle)
	<0					$x_1 \in I_1, \widetilde{x}_2 \in I_3$	2	E_1 (anti-saddle), $\widetilde{E}_2$ (saddle)
						$x_1 \notin I_1, \widetilde{x}_2 \in I_3$	1	$\widetilde{E}_2$ (saddle)
	$=0$	<0				$x_1 = \widetilde{x}_1 = n, \widetilde{x}_2 \in I_3$	2	E_n, $\widetilde{E}_2$ (saddle)
		$=0$				$x_1 = \widetilde{x}_* = n = \frac{1}{2}$	1	E_n
		>0				$x_2 = \widetilde{x}_2 = n, x_1 \in I_1$	2	E_1 (anti-saddle), E_n
						$x_1 = \widetilde{x}_2 = n$	1	E_n
						$x_* = \widetilde{x}_2 = n$	1	E_n

5 Bifurcation analysis of the full system (1.2)

5.1 Bogdanov–Takens bifurcation of codimension 3 around E_*

In the Case (II)(ii) of Theorem 2.2, we know that system (1.2) may exhibit Bogdanov–Takens bifurcation of codimension 3 around $E_*(x_*, y_*)$. In this section, we explore rigorously if a Bogdanov–Takens bifurcation of codimension 3 can be fully unfolded inside the class of system (1.2).

Let

$$\Gamma = \Gamma_{11} \cup \Gamma_{12} \cup \Gamma_{13}, \tag{5.1}$$

where

$$\begin{aligned}
\Gamma_{11} = \Big\{&(a,\, b,\, c,\, d,\, n,\, x_*) : a = a_0,\, b = b_0,\, d = d_0,\, c = \bar{c}_1,\\
&\max\{c,\, \frac{1}{2}\} < x_* < \min\{n,\, \frac{1}{4}\left(1+\sqrt{2}\right),\, \frac{1+c}{2}\}\Big\},\\
\Gamma_{12} = \Big\{&(a,\, b,\, c,\, d,\, n,\, x_*) : a = a_0,\, b = b_0,\, d = d_0,\, c = \bar{c}_2,\\
&\max\{c,\, \frac{1}{2}\} < x_* < \min\{n,\, \frac{1}{4}\left(1+\sqrt{2}\right),\, \frac{1+c}{2}\}\Big\},\\
\Gamma_{13} = \Big\{&(a,\, b,\, c,\, d,\, n,\, x_*) : a = a_0,\, b = b_0,\, d = d_0,\, c = \frac{1}{2\sqrt{2}},\, x_* = \frac{1+\sqrt{2}}{4} < n\Big\},
\end{aligned}$$

in which a_0, b_0, d_0, $\bar{c}_1$ and $\bar{c}_2$ are given in (2.8), (2.9) and (2.10), respectively.

We choose b, c and d as bifurcation parameters and obtain the following unfolding system

$$\begin{aligned}
\frac{dx}{dt} &= ax(1-x) - xy - (b + r_1),\\
\frac{dy}{dt} &= y(x - c - r_2) - d - r_3,
\end{aligned} \tag{5.2}$$

where $(a,\, b,\, c,\, d,\, n,\, x_*) \in \Gamma$ and $(r_1, r_2, r_3) \sim (0, 0, 0)$.

Theorem 5.1 *When $(a,\, b,\, c,\, d,\, n,\, x_*) \in \Gamma$, system (1.2) has a unique equilibrium $E_*(x_*, y_*)$, which is a nilpotent cusp of codimension 3. If we choose b, c, and d as bifurcation parameters, then system (1.2) can undergo a Bogdanov–Takens bifurcation of codimension 3 in a small neighborhood of E_*. More precisely, there exist a series of bifurcations with lower codimension which are subordinate to the cusp E_* of codimension 3, such as:*

(I) *Codimension 1: Hopf bifurcation, homoclinic bifurcation, saddle-node bifurcation of limit cycles, saddle-node bifurcation;*
(II) *Codimension 2: degenerate Hopf bifurcation, Bogdanov–Takens bifurcation, degenerate homoclinic bifurcation, Hopf and homoclinic bifurcations simultaneously.*

Proof We first make the following transformations successively

$$X = x - x_*,\ Y = y - y_*;$$
$$X_1 = X,\ Y_1 = \frac{dX}{dt};$$

system (1.3) becomes as

$$\begin{aligned}\frac{dX_1}{dt} &= Y_1,\ \frac{dY_1}{dt} = c_{00} + c_{10}X_1 + c_{01}Y_1 + c_{20}X_1^2 + c_{11}X_1Y_1\\ &+ c_{02}Y_1^2 + c_{30}X_1^3 + c_{21}X_1^2Y_1\\ &+ c_{12}X_1Y_1^2 + c_{40}X_1^4 + c_{31}X_1^3Y_1 + c_{22}X_1^2Y_1^2 + O(|X_1, Y_1|^5),\end{aligned} \tag{5.3}$$

where c_{ij} can be expressed by x_*, r_1, r_2 and r_3, we omit them for brevity.

Now following the similar steps in Xiang et al. (2020), Huang et al. (2016), Li et al. (2015), and performing a sequence of near-identity transformations and time rescaling (preserving orientations of orbits), we can reduce system (5.3) to the following form:

$$\begin{aligned}\frac{dX_2}{dt} &= Y_2,\\ \frac{dY_2}{dt} &= \mu_1 + \mu_2Y_2 + \mu_3X_2Y_2 + X_2^2 - X_2^3Y_2 + R(X_2, Y_2, r),\end{aligned} \tag{5.4}$$

where $R(X_2, Y_2, r) = Y_2^2O(|X_2, Y_2|^2)+O(|X_2, Y_2|^5)+O(r)(O(Y_2^2)+O(|X_2, Y_2|^3))+O(r^2)O(|X_2, Y_2|)$.

With the help of Mathematica software, when $(a, b, c, d, n, x_*) \in \Gamma_{11}$, Γ_{12} and Γ_{13}, we can obtain $\left|\frac{\partial(\mu_1,\mu_2,\mu_3)}{\partial(r_1,r_2,r_3)}\right|_{r=0} = G_1$, G_2 and G_3, respectively,

$$\begin{aligned}G_1 &= -2x_*^{-\frac{1}{5}}K_1^{-\frac{12}{5}}(w_1 + 4x_* + 1)^4(w_1 + 8x_* - 3)^3(w_1 - 16x_*^2 + 4x_* + 1)^{\frac{4}{5}},\\ G_2 &= 2x_*^{-\frac{1}{5}}K_2^{-\frac{12}{5}}(w_1 - 4x_* - 1)^4(w_1 - 8x_* + 3)^3(w_1 + 16x_*^2 - 4x_* - 1)^{\frac{4}{5}},\\ G_3 &= -\frac{4096\cdot 2^{2/5}\left(-41 - 29\sqrt{2}\right)^{4/5}\left(2 + 3\sqrt{2}\right)^{24/5}\left(650 + 457\sqrt{2}\right)}{\left(\sqrt{2} - 4\right)^4\left(1 + \sqrt{2}\right)^{37/5}\left(58 + 45\sqrt{2}\right)^3} \neq 0,\end{aligned}$$

where w_1 is given in (2.17), and

$$\begin{aligned}K_1 &= w_1k_{11} + k_{12},\\ K_2 &= w_1k_{11} - k_{12},\\ k_{11} &= 576x_*^5 - 960x_*^4 + 312x_*^3 - 4x_*^2 - 10x_* + 1,\\ k_{12} &= 3328x_*^6 - 2112x_*^5 - 672x_*^4 + 520x_*^3 - 60x_*^2 - 6x_* + 1.\end{aligned}$$

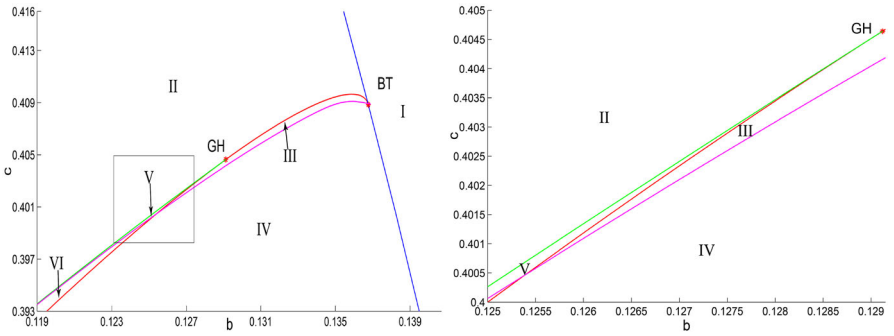

Fig. 4 **a** Bifurcation diagram for system (1.3) in $(b,\ c)$ plane when $a = 0.7, d = 0.01$. BT and GH denote the Bogdanov–Takens bifurcation point and degenerate Hopf bifurcation point, respectively. Blue, purple, red and green curves denote saddle-node bifurcation, homoclinic bifurcation, Hopf bifurcation, saddle-node bifurcation of limit cycles, respectively. **b** The local enlarged view of (**a**)

In fact, since $\frac{1}{2} < x_* < \frac{1+\sqrt{2}}{4}$, it is easy to see that $w_1 - 4x_* - 1 < 0$, $w_1 + 8x_* - 3 > 0$, $w_1 - 8x_* + 3 < 0$, $16x_*^2 - 4x_* - 1 > 0$, $w_1 - 16x_*^2 + 4x_* + 1 < 0$. We next discuss the signs of K_1 and K_2. By applying Sturm's theorem, we know that k_{11} and k_{12} have no real root in $(\frac{1}{2}, \frac{1+\sqrt{2}}{4})$. From $k_{11}|_{x_*=\frac{1}{2}} = -8$ and $k_{12}|_{x_*=\frac{1}{2}} = -8$ it follows that $k_{11} < 0$ and $k_{12} < 0$, thus $K_1 < 0$. Moreover, by $k_{12}^2 - (w_1 k_{11})^2 = 16384x_*^6(10x_*^2 - 7x_* + 1)^3 > 0$, we have $K_2 > 0$. From the above discussion, we conclude that $\left|\frac{\partial(\mu_1,\mu_2,\mu_3)}{\partial(r_1,r_2,r_3)}\right|_{r=0} \neq 0$ if $(a,\ b,\ c,\ d,\ n,\ x_*) \in \Gamma$.

Therefore, by the results of Dumortier et al. (1987) and Chow et al. (1994), we know that system (5.4) is the versal unfolding of a Bogdanov–Takens singularity (cusp case) of codimension 3. The remainder term $R(X_2, Y_2, r)$ has no influence on the bifurcations and dynamics. □

Remark 5.2 Fixing $(a, d) = (0.7, 0.01)$ and using the program Matcont, we get Fig. 4, which is a 2-parameter bifurcation diagram in the (b, c)-plane. The BT and GH in Fig. 4 denote the Bogdanov–Takens bifurcation point and degenerate Hopf bifurcation point, respectively. Blue, purple, red and green curves denote saddle-node bifurcation, homoclinic bifurcation, Hopf bifurcation, saddle-node bifurcation of limit cycles, respectively. The bifurcation curves divide the (b, c)-plane into 6 regions, system (1.2) undergoes a series of bifurcations and exhibits abundant dynamics when parameters vary in these regions (see phase portraits in Fig. 5). Table 5 shows the detailed dynamical behaviors of system (1.2) in subregions $I - VI$ of Fig. 4.

5.2 Hopf bifurcation around E_1 of system (1.2)

In this subsection, we discuss Hopf bifurcation around $E_1(x_1, y_1)$ in system (1.2). Since $E_1(x_1, y_1)$ locates in the region D_1 and the limit cycles arising from the Hopf

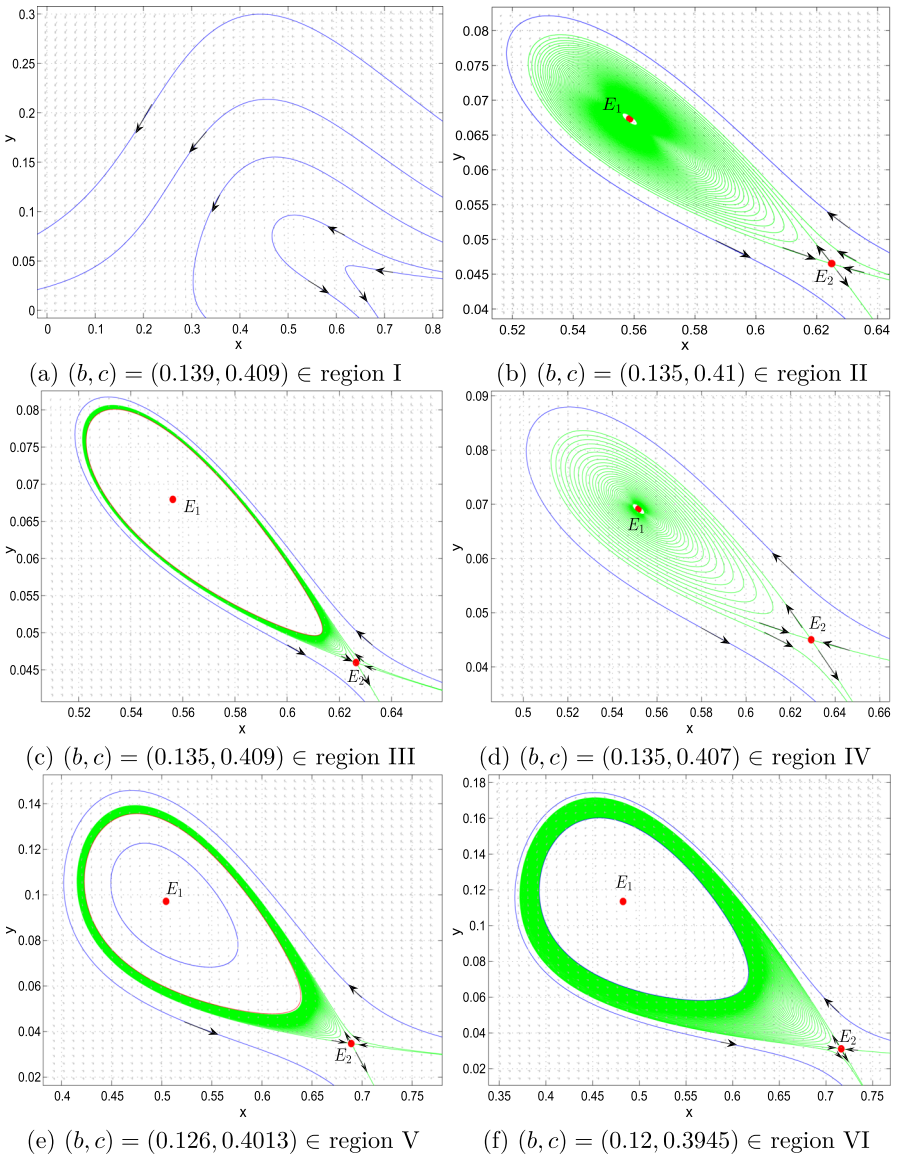

Fig. 5 Phase portraits of system (1.3) with (b, c) located in different subregions of Fig. 4, $n = 1$, $a = 0.7$ and $d = 0.01$. The detailed dynamical behaviors are described in Table 5

bifurcation are small-amplitude, we can actually discuss Hopf bifurcation around E_1 in system (1.3).

From $f(x_1) = 0$ and $\mathrm{Tr}(J(E_1)) = 0$, we can get $b = b^H$ and $d = d^H$, where d^H was defined in (2.18) and $b^H := x_1[c + (a - 1)x_1]$. Further, when $b = b^H$ and $d = d^H$, we have $\mathrm{Det}(J(E_1)) = ax_1(1 - 2x_1) + c(x_1 - c)$. From $b^H > 0$, $d^H > 0$

Table 5 The dynamical behaviors of system (1.2) in different subregions of Fig. 4

Region: phase portrait	Equilibrium	Limit cycle	
		Number	Stability
I: Fig. 5a	No	0	
II: Fig. 5b	E_1: Ⓢ E_2: Ⓤ	0	
III: Fig. 5c	E_1: Ⓤ E_2: Ⓤ	1	Ⓢ
IV: Fig. 5d	E_1: Ⓤ E_2: Ⓤ	0	
V: Fig. 5e	E_1: Ⓢ E_2: Ⓤ	2	Inner: Ⓤ outer: Ⓢ
VI: Fig. 5f	E_1: Ⓢ E_2: Ⓤ	1	Ⓤ

Notation Ⓢ (resp. Ⓤ) represents stable (resp. unstable) positive equilibrium or limit cycle

and $\mathrm{Det}(J(E_1)) > 0$, we immediately get $(c,\ a,\ x_1) \in \Lambda$, where

$$\Lambda := \left\{0 < c < 1,\ \max\left\{\frac{1}{2},\ c\right\} < x_1 < \frac{c+1}{2},\ 1 - \frac{c}{x_1} < a < \frac{c(c-x_1)}{x_1(1-2x_1)}\right\} \cup \left\{c < \frac{1}{2},\ c < x_1 \le \frac{1}{2},\ a > 1 - \frac{c}{x_1}\right\}. \tag{5.5}$$

Hence, we have the following result.

Theorem 5.3 *When $b = b^H$, $d = d^H$ and $(c,\ a,\ x_1) \in \Lambda$, $E_1(x_1, y_1)$ is a weak focus of order at most two.*

Proof When $b = b^H$ and $d = d^H$, we transform $E_1(x_1, y_1)$ into the origin by letting $X = x - x_1$, $Y = y - y_1$, where $y_1 = \frac{d^H}{x_1 - c}$, then system (1.3) becomes (still denote X, Y by x, y respectively)

$$\begin{aligned} \frac{dx}{dt} &= (c - x_1)x - x_1 y - ax^2 - xy + o(|x, y|^5), \\ \frac{dy}{dt} &= [a\,(1 - 2x_1) - c + x_1]x + (x_1 - c)y + xy + o(|x, y|^5). \end{aligned} \tag{5.6}$$

Then making a change of variables as $x = X$, $y = \frac{c - x_1}{\omega} X - \frac{\omega}{x_1} Y$ and $\tau = \omega t$ where

$$\omega = \sqrt{ax_1\,(1 - 2x_1) - c^2 + cx_1}.$$

We can rewrite system (5.6) as (still denote X, Y by x, y, respectively)

$$\begin{aligned} \frac{dx}{dt} &= y + \frac{x_1 - c - ax_1}{x_1\omega}x^2 + \frac{1}{x_1}xy + o(|x, y|^5), \\ \frac{dy}{dt} &= -x - \frac{(c - x_1)(c + ax_1)}{x_1\omega^2}x^2 + \frac{c}{x_1\omega}xy + o(|x, y|^5). \end{aligned} \tag{5.7}$$

Using the formal series method in Zhang et al. (1992) and Mathematica software, when $b = b^H$ and $d = d^H$, we obtain the first two Lyapunov coefficients as follows:

$$L_1 := \frac{f_1(c, a, x_1)}{-4x_1\omega^3},\ L_2 := \frac{f_2(c, a, x_1)}{-96x_1^3\omega^7}, \tag{5.8}$$

where

$$\begin{aligned}
f_1(c, a, x_1) &= a^2x_1(-2c + 4x_1 - 1) + a((6c + 1)x_1 - c(2c + 1) - 4x_1^2) + c(c - x_1),\\
f_2(c, a, x_1) &= -124a^5(x_1^4(2x_1 - 1)(2c - 4x_1 + 1)) - a^4x_1^3(228c^3 + (512c^2 + 2370c + 339)x_1\\
&\quad - 474c^2 - 8(423c + 262)x_1^2 - 292c + 2848x_1^3 + 1) + a^3x_1^2((1382c^2 + 3927c + 339)x_1^2\\
&\quad + (1354c^3 - 2013c^2 - 551c + 1)x_1 + c(-528c^3 + 170c^2 + 215c - 1) - 4(1261c\\
&\quad + 524)x_1^3 + 2848x_1^4) + a^2x_1(2(195c^2 - 970c - 62)x_1^3 + c(-3164c^2 + 1498c + 295)x_1^2\\
&\quad + 2c^2(1053c^2 - 105c - 109)x_1 + c^3(-372c^2 - 92c + 47) + 8(254c + 93)x_1^4 - 992x_1^5)\\
&\quad + ac(-36c^4(2c + 1) + 2c^3(388c + 93)x_1 - c^2(2361c + 263)x_1^2 - 1519cx_1^4 + c(2928c\\
&\quad + 113)x_1^3 + 248x_1^5) + c^2(c - x_1)^2(36c^2 - 161cx_1 + 124x_1^2).
\end{aligned}$$

Let the algebraic variety $V(\xi_1, \xi_2, \ldots, \xi_n)$ denote the set of common zeros of ξ_i $(i = 1, 2, \ldots n)$, $\mathrm{res}(f, g, x)$ denote the Sylvester resultant of f and g with respect to x, $\mathrm{lcoeff}(f, x)$ denote the leading coefficient of the polynomial f with respect to x, $\mathrm{prem}(\xi, \eta, x)$ denote the preudoreminder of ξ divided by η with respect to x. Compute the resultant

$$\mathrm{res}(f_1, f_2, a) = 16c^4x_1^6(c - x_1)^3R_1R_2^2R_3^2R_4,$$

where

$$\begin{aligned}
R_1 &= 2c - 4x_1 + 1,\\
R_2 &= c - 3x_1 + 1,\\
R_3 &= 2c^2 - 4cx_1 + c + 4x_1^2 - 2x_1,\\
R_4 &= 8c^2 - 31cx_1 + 4c + 21x_1^2 - 3x_1.
\end{aligned}$$

Decomposing $V(f_1, f_2) \cap \Lambda$ into three subsets. By Lemma 2 in Chen and Zhang (2009), we have the decomposition

$$V(f_1, f_2) \cap \Lambda = (V(f_1, f_2, \mathrm{lcoeff}(f_1, a)) \cap \Lambda) \cup (V(\frac{f_1, f_2, \mathrm{res}(f_1, f_2, a)}{\mathrm{lcoeff}(f_1, a)}) \cap \Lambda).$$

Since $\mathrm{lcoeff}(f_1, a) = -x_1R_1$, from $R_1 = 0$, we have $c = \widetilde{c_1} = \frac{4x_1-1}{2}$. To guarantee parameter conditions, we have $\widetilde{c_1} > 0$ and $x_1 > \widetilde{c_1}$, i.e., $\frac{1}{4} < x_1 < \frac{1}{2}$.

Further $f_1|_{c=\widetilde{c_1}} = \frac{1}{4}(2x_1-1)(4x_1-1) \neq 0$, then $V(f_1, R_1) \cap \Lambda = \emptyset$, thus $V(f_1, f_2, \text{lcoeff}(f_1, a)) \cap \Lambda = \emptyset$. Therefore,

$$\begin{aligned} V(f_1, f_2) \cap \Lambda &= V(f_1, f_2, \text{res}(f_1, f_2, a)) \cap \Lambda \\ &= V(f_1, f_2, R_2R_3R_4) \cap \Lambda \\ &= (V(f_1, f_2, R_2) \cap \Lambda) \cup (V(f_1, f_2, R_3) \cap \Lambda) \cup (V(f_1, f_2, R_4) \cap \Lambda). \end{aligned} \tag{5.9}$$

We now prove $V(f_1, f_2) \cap \Lambda = \emptyset$ in three steps.

Step 1: we prove $V(f_1, f_2, R_2) \cap \Lambda = \emptyset$. From $R_2 = 0$ we get $c = \widetilde{c_2} = 3x_1 - 1$. Since $\widetilde{c_2} > 0$ and $x_1 > \widetilde{c_2}$, we have $\frac{1}{3} < x_1 < \frac{1}{2}$. Further

$$f_1|_{c=\widetilde{c_2}} = (1-a)\,(2x_1-1)\,[(a+3)x_1 - 1]\,.$$

If $f_1|_{c=\widetilde{c_2}} = 0$, then $a = 1$. However,

$$f_2|_{c=\widetilde{c_2}, a=1} = 16x_1\,(2x_1-1)^{\,2}\,(3x_1-1)\,(4x_1-1)^{\,2} \neq 0,$$

since $\frac{1}{3} < x_1 < \frac{1}{2}$. Thus $V(f_1, f_2, R_2) \cap \Lambda = \emptyset$.

Step 2: we prove $V(f_1, f_2, R_3) \cap \Lambda) = \emptyset$. Let

$$\begin{aligned} w_2 &= \text{prem}(f_2, f_1, a) \\ &= 4c^2R_1^2(c-x_1)^2x_1^5k_{21} + 4acR_1^3(c-x_1)x_1^5k_{22} \\ &= 4cR_1^2(c-x_1)x_1^5[c(c-x_1)k_{21} + aR_1k_{22}] \\ &= 4cR_1^2(c-x_1)x_1^5\bar{w}_2, \end{aligned}$$

where

$$\begin{aligned} \bar{w}_2 &= c(c-x_1)k_{21} + aR_1k_{22}, \\ k_{21} &= x_1[4x_1(-3c+7x_1-8) + c(17-10c) + 11] + (c-1)(2c+1)(3c+1), \\ k_{22} &= x_1\{x_1[4x_1(-15c+7x_1-8) + 6c(8c+9) + 11] - (2c+1)[c(7c+12)+1]\} \\ &\quad + c(2c+1)(c+1)^2. \end{aligned}$$

Since $V(f_1, R_1) \cap \Lambda = \emptyset$, we have

$$\begin{aligned} V(f_1, f_2) \cap \Lambda &= \Big(V(f_1, f_2, \text{lcoeff}(f_1, a)) \cup V(\frac{f_1, w_2}{\text{lcoeff}(f_1, a)})\Big) \cap \Lambda \\ &= \Big(V(f_1, f_2, R_1) \cup V(\frac{f_1, w_2}{R_1})\Big) \cap \Lambda \\ &= V(f_1, \bar{w}_2) \cap \Lambda. \end{aligned}$$

Thus,

$$\begin{aligned} V(f_1, f_2, R_3) \cap \Lambda &= V(f_1, f_2) \cap V(R_3) \cap \Lambda \\ &= V(f_1, \bar{w}_2) \cap V(R_3) \cap \Lambda \\ &= V(f_1, \bar{w}_2, R_3) \cap \Lambda. \end{aligned} \tag{5.10}$$

From $R_3 = 0$ we get $x_1 = x_{01} = \frac{1}{4}\left(\sqrt{1-4c^2} + 2c + 1\right)$ and $0 < c < \frac{1}{2}$, and it is easy to see that $x_{01} > \frac{1}{2}$. Furthermore, from $\bar{w}_2 = 0$ we have $a = a_1(c, x_1) = -\frac{c(c-x_1)k_{21}}{R_1 k_{22}}$. Moreover,

$$[a_1(c, x_1) - \frac{c(c-x_1)}{x_1(1-2x_1)}]\,|_{x_1=x_{01}} = 0,$$

thus we conclude that $V(\bar{w}_2, R_3) \cap \Lambda = \emptyset$, from (5.10) it follows that $V(f_1, f_2, R_3) \cap \Lambda = \emptyset$.

Step 3: we prove $V(f_1, f_2, R_4) \cap \Lambda = \emptyset$. Similar to the step 2, we can get

$$V(f_1, f_2, R_4) \cap \Lambda = V(f_1, \bar{w}_2, R_4) \cap \Lambda.$$

From $R_4 = 0$ we get $x_1 = x_{02}$ or $x_1 = x_{03}$ and $c \in (0, \widetilde{c_3}) \cup (\widetilde{c_4}, 1)$, where

$$x_{02} = \frac{1}{42}\left(-\sqrt{289c^2 - 150c + 9} + 31c + 3\right),\ x_{03} = \frac{1}{42}\left(\sqrt{289c^2 - 150c + 9} + 31c + 3\right),$$
$$\widetilde{c_3} = \frac{3}{289}\left(25 - 4\sqrt{21}\right),\ \widetilde{c_4} = \frac{3}{289}\left(25 + 4\sqrt{21}\right).$$

Since

$$\begin{aligned} \left(a_1(c, x_1) - (1 - \frac{c}{x_1})\right)\Big|_{x_1=x_{02}} &= -\frac{14c}{-\sqrt{289c^2 - 150c + 9} + 31c + 3} < 0, \\ \left(a_1(c, x_1) - (1 - \frac{c}{x_1})\right)\Big|_{x_1=x_{03}} &= -\frac{14c}{\sqrt{289c^2 - 150c + 9} + 31c + 3} < 0, \end{aligned}$$

we have $V(\bar{w}_2, R_4) \cap \Lambda = \emptyset$. Thus $V(f_1, f_2, R_4) \cap \Lambda = \emptyset$.

From the above discussion and (5.9), we get $V(f_1, f_2) \cap \Lambda = \emptyset$, which leads to the conclusion. □

We choose $x_1 = \frac{2}{5}$, $c = \frac{1}{5}$ and $a = 1$, then $f_1 = 0$ (i.e., $L_1 = 0$), $f_2 \doteq 0.018432 > 0$, $b^H = \frac{2}{25}$ and $d^H = \frac{2}{25}$. By direct calculation we obtain that $\left|\frac{\partial(\mathrm{Tr}(J(E_1)), L_1)}{\partial(d, a)}\right|_{a=1, b=\frac{2}{25}, c=\frac{1}{5}, d=\frac{2}{25}} = \frac{125}{8\sqrt{3}} \neq 0$. Then we have the following theorem.

Theorem 5.4 *Suppose that $x_1 < n$, $(a, c, x_1) \in \Lambda$ and $d = d^H$.*

(i) *If $f_1 < 0$, then there is one unstable limit cycle in system (1.2) as d increases from d^H;*

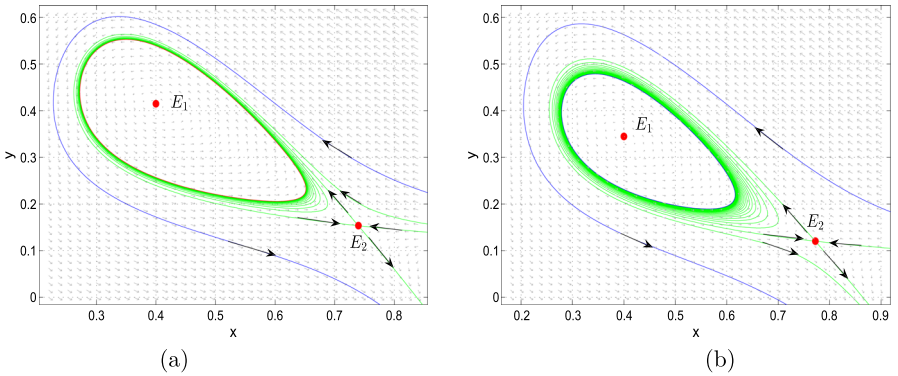

Fig. 6 **a** A stable limit cycle generated by the supercritical Hopf bifurcation with $a = \frac{11}{10}, b = \frac{49}{500}, c = \frac{1}{5}$, $d = \frac{83}{1000}, n = 1$; **b** an unstable limit cycle created by the subcritical Hopf bifurcation with $a = \frac{7}{10}$, $b = \frac{3}{100}, c = \frac{1}{5}, d = \frac{69}{1000}, n = 1$. Where $E_1, E_2 \in D_1$

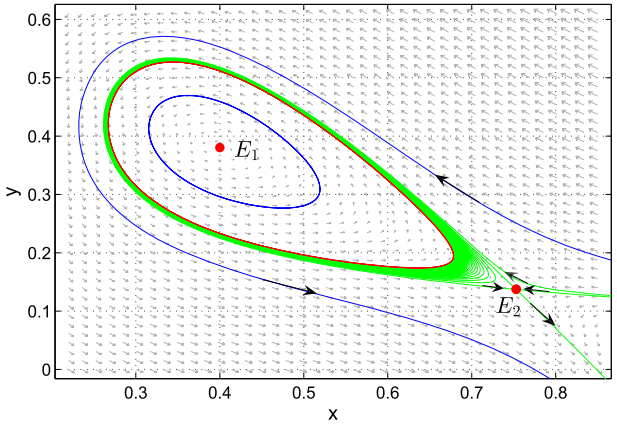

Fig. 7 Two limit cycles (the inner one is unstable and the outer is stable) generated by degenerate Hopf bifurcation in system (1.2) with $a = \frac{9}{10}, b = \frac{319}{5000}, c = \frac{1}{5}, d = \frac{761}{10000}, n = 1$. Where $E_1, E_2 \in D_1$

(ii) *If $f_1 = 0$, then there are two limit cycles in system (1.2) as d increases from d^H and f_1 decreases from 0, the inner is unstable, and the outer is stable;*

(iii) *If $f_1 > 0$, then there is one stable limit cycle in system (1.2) as d decreases from d^H.*

In Fig. 6, by incorporating the above analysis and using numerical simulations we present the existence of one limit cycle generated by the supercritical and subcritical Hopf bifurcations of codimension 1. In Fig. 7, we show the degenerate Hopf bifurcation and the existence of two limit cycles, where the unstable one is in the interior of the stable one.

6 Existence of multiple limit cycles in the full system (1.2)

In this section, by numerical simulations we give some portraits of system (1.2) for different parameters. From Fig. 8a–c, it is evident that when system (1.2) has an equilibrium on each side of line $x = n$, it can display supercritical Hopf bifurcation of codimension 1, subcritical Hopf bifurcation of codimension 1 and degenerate Hopf bifurcation, respectively. Surprisingly, from Fig. 8d, we can see that system (1.2) can exhibit the coexistence of an unstable limit cycle and a semi-stable limit cycle. Figure 8e shows that system (1.2) can exhibit three limit cycles, in which the outermost and innermost limit cycles are unstable and the middle one is stable.

7 Summary and discussion

To study the effects of whaling and krill fishing on the population dynamics of the krill–whale interaction and to explore the so-called krill paradox phenomenon, in this paper we considered a predator–prey model (1.1) with Holling type I functional response in which both predator and prey are harvested with constant-yield harvesting. Dai and Tang (1998) found that the maximum safe harvest may be far less than what would be assumed from a local analysis of equilibria. Further, they proved that model (1.1) can exhibit complex dynamics, such as the existence of multiple limit cycles and homoclinic orbits, by using qualitative analysis and Poincaré-Bendixson theorem. However, they only focused on the case that there exists one positive equilibrium on each side of $N = 2N_c$.

In this paper, we mainly investigated the bifurcation of equilibria which locate in the region $N < 2N_c$. After performing a detailed qualitative and bifurcation analysis, our results reveal that system (1.2) (i.e. (1.1)) exhibits complex dynamics and bifurcations such as the existence of a nilpotent cusp of codimension 3 and a weak focus of multiplicity at most 2 and up to 2 for variously parameter values, and system (1.2) undergoes a sequence of bifurcations including cusp type degenerate Bogdanov–Takens bifurcation of codimension 3, Hopf bifurcation and degenerate Hopf bifurcation of codimension at most and up to 2 as the parameters vary. More precisely, there exist a series of bifurcations with lower codimension which are subordinate to a cusp of codimension 3, including (i) codimension 1: Hopf bifurcation, homoclinic bifurcation, saddle-node bifurcation of limit cycles, saddle-node bifurcation; (ii) codimension 2: degenerate Hopf bifurcation, Bogdanov–Takens bifurcation, degenerate homoclinic bifurcation, Hopf and homoclinic bifurcations simultaneously. Therefore, system (1.2) can exhibit the coexistence of a stable homoclinic loop and an unstable limit cycle, coexistence of two limit cycles (the inner one unstable), and a semi-stable limit cycle for different sets of parameters. Moreover, numerical simulation reveals that system (1.1) can have three limit cycles under specific parameters, and the coexistence of an unstable limit cycle and a semi-stable limit cycle under different parameters. Our results can be seen as a theoretical complement to the work by Dai and Tang (1998).

As for the "krill paradox" phenomenon in Fig. 1a, simulations indicate on the left of the eqilibrium E_n in Fig. 3a–c, e and on the left of the equilibrium E_1 in Fig. 3d,

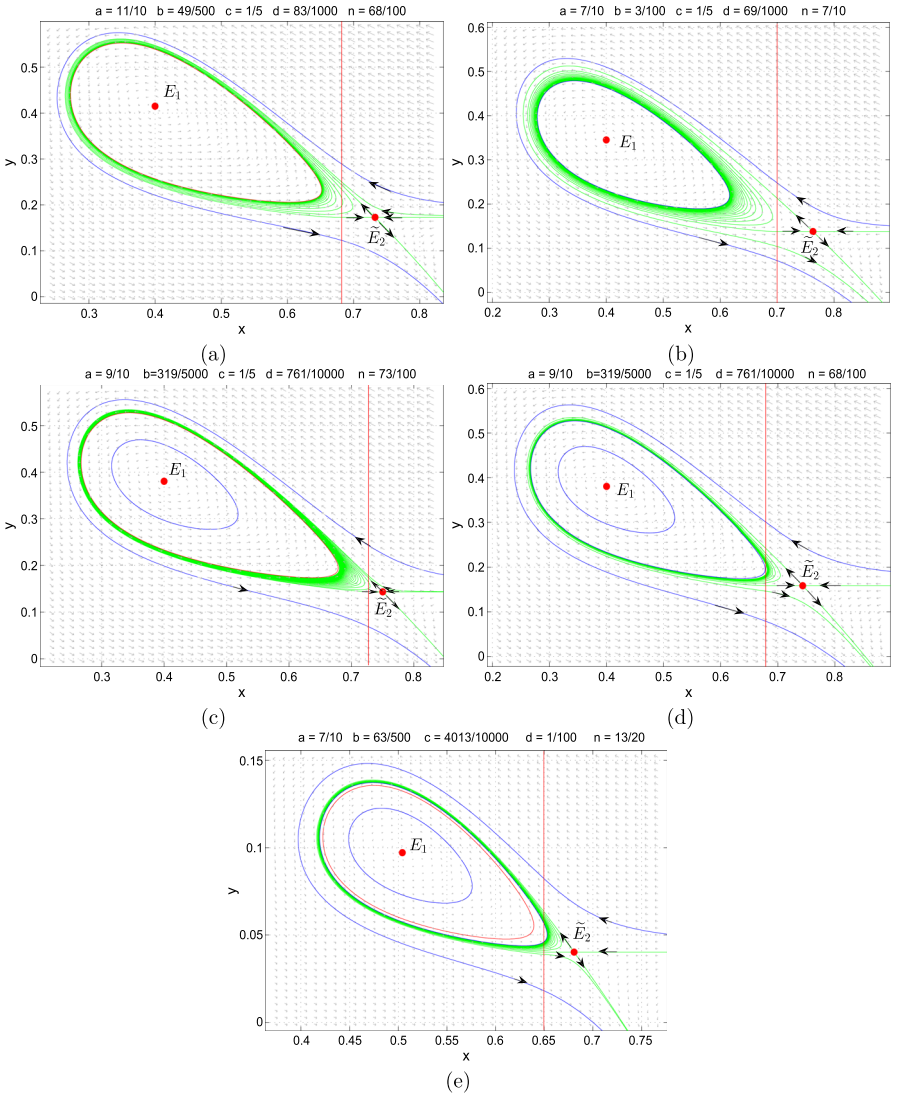

Fig. 8 Multiple limit cycles in system (1.2) with $E_1 \in D_1$ and $\widetilde{E}_2 \in D_2$. **a** A stable limit cycle; **b** an unstable limit cycle; **c** two limit cycles (the inner one is unstable and the outer stable); **d** two limit cycles (the inner one is unstable and the outer is semi-stable); **e** three limit cycles (the outermost and innermost limit cycles are unstable and the middle one is stable)

both prey (krill) and predator (whale) populations decrease. Also, on the left of the equilibrium in Fig. 8a, both components decrease.

The obtained bifurcation results (Theorems 5.1–5.4, Figs. 4, 5, 6, 7) of system (1.2) indicate that the dynamical behaviors, such as extinction, coexistence and oscillation of both species, are highly sensitive to both the environment parameters (such as the harvesting constants) and the initial density of two species. This implies the need for

meticulous resource management and harvesting policies in the context of conservation and renewable applications (see Ruan and Xiao 2023). In fact, in Theorems 5.1, the bifurcation parameters b, c and d depend on the harvesting parameters h_1, h_2 and other original environment parameters, when (b, c, d) vary around the bifurcation value $(b_0, \bar{c}_1, d_0)$ (or $(b_0, \bar{c}_2, d_0)$, or $(b_0, \frac{1}{2\sqrt{2}}, d_0)$), the dynamics and the fate of both species can change dramatically. For example, in Fig. 5a, predator or prey will tend to extinction for all positive initial densities; in Fig. 5b, both species will tend to a stable steady state E_1 under some positive initial densities, while one of species will tend to extinction for other positive initial densities; in Fig. 5c, both species will tend to a stable periodic oscillation for initial densities between the two stable manifolds of E_2 or inside the stable limit cycle, while one of species will tend to extinction for other positive initial densities; in Figs. 5d, one of species will tend to extinction for almost all positive initial densities; in Fig. 5e, there exist bistability (E_1 and the outer limit cycle) and two periodic oscillations with different periods and amplitudes, both species will tend to the stable steady state E_1 or the stable oscillation for some positive initial densities; in Fig. 5f, there exists one unstable periodic oscillation, both species will tend to the stable steady state E_1 for some positive initial densities. Figure 7 undergoes similar properties. On the other hand, system (1.1) is uniformly persistent if $h_1 = h_2 = 0$ (Dai and Tang 1998). However, for $h_1 > 0$ and $h_2 > 0$, solutions of system (1.1) with positive initial values may cross the coordinate axis and leave the first quadrant (for example see Fig. 5a), which means that the species with positive initial densities will tend to extinction.

Since seasonal change and spatial variation are important in studying population dynamics of krill and whales, it would be interesting to incorporate such features in the krill–whale predation models. Moreover, krill and whales are parts of the ocean food chain, it would be very challenging to investigate the effects of fishing on food chains. Finally, although we have explored the equilibrium E_n on the line $x = n$ in Theorem 4.1 and Figs. 3 and 8, the detailed dynamics (such as crossing limit cycles in Figure) and bifurcations need more techniques and methods for piecewise-smooth systems. We leave these for future consideration.

Acknowledgements We would like to thank the two anonymous reviewers for their helpful comments and valuable suggestions. Research of J. Huang was partially supported by NSFC (No. 12231008). Research of S. Ruan was partially supported by National Science Foundation (DMS-2052648).

Data availibility This paper has no associated data.

Declarations

Conflicts of interest The authors declare that they have no conflict of interest.

References

Beddington JR, May RM (1980) Maximum sustainable yields in systems subject to harvesting at more than one trophic level. Math Biosci 51:261–281

Beddington JR, May RM (1982) The harvesting of interacting species in a natural ecosystem. Sci Am 247(5):62–69
Brauer F, Soudack AC (1979) Stability regions in predator–prey systems with constant-rate prey harvesting. J Math Biol 8:55–71
Brauer F, Soudack AC (1981) Coexistence properties of some predator–prey systems under constant rate harvesting and stocking. J Math Biol 12:101–114
Butterworth DS, Thomson RB (1995) Possible effects of different levels of krill fishing on predators some initial modelling attempts. CCAMLR Sci 2:79–97
Chen X, Zhang W (2009) Decomposition of algebraic sets and applications to weak centers of cubic systems. J Comput Appl Math 232(2):565–581
Chen J, Huang J, Ruan S, Wang J (2013) Bifurcations of invariant tori in predator–prey models with seasonal prey harvesting. SIAM J Appl Math 73:1876–1905
Chow S-N, Li C, Wang D (1994) Normal forms and bifurcation of planar vector fields. Cambridge University Press, Cambridge
Dai G, Tang M (1998) Coexistence region and global dynamics of a harvested predator–prey system. SIAM J Appl Math 58:193–210
Dai G, Xu X (1991) Constant rate prey harvested predator-prey system with Holling-type I functional response. J Biomath 6:155–162 (**in Chinese**)
Dai G, Xu X (1994) Constant rate predator harvested predator-prey system with Holling type I functional response. Acta Math Sci 14:134–144 (**in Chinese**)
Dubois DM, Closset PL (1975) Patchiness in primary and secondary production in the Southern Bight: a mathematical theory. In: Proceedings of the 10th European symposium on marine biology, vol 2. Belgium Universal Press, Wetteren, pp 211–229
Dumortier F, Roussarie R, Sotomayor J (1987) Generic 3-parameter families of vector fields on the plane, unfolding a singularity with nilpotent linear part. The cusp case of codimension 3. Ergod Theory Dyn Syst 7(3):375-413
Freedman HI (1980) Deterministic mathematical models in population ecology. Marcel Dekker, New York
Hill SL, Murphy EJ, Reid K, Trathan PN, Constable AJ (2006) Modelling Southern Ocean ecosystems: krill, the food-web, and the impacts of harvesting. Biol Rev 81:581–608
Hofman RJ (2017) Sealing, whaling and krill fishing in the Southern Ocean: past and possible future effects on catch regulations. Polar Rec 53(268):88–99
Holling CS (1959) The functional response of predators to prey density and its role in mimicry and population regulation. Mem Entomol Soc Can 91(45):385–398
Horwood JW (1981) On the joint exploitation of krill and whales. In: Mammals in the Seas. FAO, Rome, pp 363–368
Huang J, Gong Y, Ruan S (2013) Bifurcation analysis in a predator–prey model with constant-yield predator harvesting. Discrete Contin Dyn Syst B 18(8):2101–2121
Huang J, Liu S, Ruan S, Zhang X (2016) Bogdanov–Takens bifurcation of codimension 3 in a predator–prey model with constant-yield predator harvesting, Commun. Pure. Appl Anal 15:1041–1055
Kawamura A (1994) A review of baleen whale feeding in the Southern Ocean. Rep Int Whaling Comm 44:261–271
Li C, Li J, Ma Z (2015) Codimension 3 B-T bifurcations in an epidemic model with a nonlinear incidence. Discrete Contin Dyn Syst B 20:1107–1116
Lu M, Huang J, Wang H (2023) An organizing center of codimension four in a predator-prey model with generalist predator: from tristability and quadristability to transients in a nonlinear environmental change. SIAM J Appl Dyn Syst 22:694–729
May RM (1973) Stability and complexity in model ecosystems. Princeton University Press, Princeton, NJ
May R, Beddington JR, Clark CW, Holt SJ, Laws RM (1979) Management of multispecies fisheries. Science 205:267–277
Mori M, Butterworth DS (2004) Consideration of multispecies interactions in the Antarctic: a preliminary model of the minke whale-blue whale-krill interaction. Afr J Mar Sci 26:245–259
Mori M, Butterworth DS (2006) A first step towards modeling the krill-predator dynamics of the Antarctic ecosystem. CCAMLR Sci 13:217–277
Perko L (2001) Differential equations and dynamical systems, 3rd edn. Springer, New York
Ren Y, Han L (1989) The predator prey model with two limit cycles. Acta Math Appl Sinica 5:30–32
Ruan S, Xiao D (2023) Imperfect and Bogdanov-Takens bifurcations in biological models: from harvesting of species to isolation of infectives. J Math Biol 87:1–26

Savoca MS, Czapanskiy MF, Kahane-Rapport SR et al (2021) Baleen whale prey consumption based on high-resolution foraging measurements. Nature 599:85–90
Seo G, DeAngelis DL (2011) A predator–prey model with a Holling type I functional response including a predator mutual interference. J Nonlinear Sci 21:811–833
Willis J (2007) Could whales have maintained a high abundance of krill? Evolut Ecol Res 9:651–662
Willis J (2014) Whales maintained a high abundance of krill; both are ecosystem engineers in the Southern Ocean. Mar Ecol Prog Ser 513:51–69
Xiang C, Huang J, Ruan S, Xiao D (2020) Bifurcation analysis in a host-generalist parasitoid model with Holling II functional response. J Differ Equ 268:4618–4662
Xiao D, Ruan S (1999) Bogdanov–Takens bifurcations in predator-prey systems with constant rate harvesting. Fields Inst Commun 21:493–506
Yamanaka I (1983) Interaction among krill, whales and other animals in the Antarctic ecosystem. Mem Natl Inst Polar Res Spec 27:220–232
Zegeling A, Kooij RE (2020) Singular perturbation of the Holling I predator–pery system with a focus. J Differ Equ 269:5434–5462
Zhang Z, Ding T, Huang W, Dong Z (1992) Qualitative Theory of Differential Equations, Transl. Math. Monogr. vol 101. American Mathematical Society, Providence
Zhang Y, Huang J, Wang H (2023) Bifurcations driven by generalist and specialist predation: mathematical interpretation of Fennoscandia phenomenon. J Math Biol 86, Article number: 94